Journal of Cellular Biochemistry 94:540–553 (2005)

S19 Ribosomal Protein Dimer Augments Metal-Induced Apoptosis in a Mouse Fibroblastic Cell Line by Ligation of the C5a Receptor

Hiroshi Nishiura,[1]* Sumio Tanase,[2] Yoko Shibuya,[3] Noriko Futa,[4] Tamami Sakamoto,[4] Adrian Higginbottom,[5] Peter Monk,[5] Jörg Zwirner,[6] and Tetsuro Yamamoto[1]

[1]Department of Molecular Pathology, Faculty of Medical and Pharmaceutical Sciences, Kumamoto University, Kumamoto, Japan
[2]Department of Medical Biochemistry, Faculty of Medical and Pharmaceutical Sciences, Kumamoto University, Kumamoto, Japan
[3]Laboratory Medicine, Faculty of Medical and Pharmaceutical Sciences, Kumamoto University, Kumamoto, Japan
[4]Trans Genic, Incorporation, Kumamoto, Japan
[5]Unit of Academic Neurology, Sheffield University Medical School, Sheffield, United Kingdom
[6]Department of Immunology, Georg-August-University, Göttingen, Germany

Abstract To analyze the role of S19 ribosomal protein (RP S19) in apoptosis, murine NIH3T3 were transfected with either hemagglutinin peptide-tagged (HA) wild-type human RP S19 or a mutant (Gln137Asn) that is resistant to transglutaminase-catalyzed cross-linked-dimerization. Transfection with the mutant HA-RP S19 inhibited manganese (II) (Mn II)-induced apoptosis whereas the wild-type HA-RP S19 augmented apoptosis and a mock transfection had no effect. Release of the wild-type HA-RP S19 dimer but not the mutant HA-RP S19 was observed during the apoptosis. The reduced rate of apoptosis of the cells transfected with the mutant HA-RP S19 was overcome by addition of extracellular wild-type RP S19 dimer. The apoptosis rates in cells transfected with either form of human HA-RP S19 and in mock transfectants were reduced to about 40% by the presence of anti-RP S19 antibody in the culture medium. Immunofluorescence staining and fluorescence-activated cell sorting (FACS) analysis showed that the cell surface expression of the receptor for cross-linked RP S19 dimer, C5a receptor, increased during apoptosis, concomitant with phosphatidylserine exposure. The expression of the C5a receptor gene also increased twofold. Apoptosis rates in the transfected and control cell lines were also reduced by the presence of an anti-mouse C5a receptor monoclonal antibody or of a peptide C5a receptor antagonist. These results indicated the presence of an RP S19 dimer- and C5a receptor-mediated autocrine-type augmentation mechanism during Mn II-induced apoptosis in the mouse fibroblastic cell line. In contrast to the RP S19 dimer, C5a actually inhibited apoptosis, suggesting that signaling through the C5a receptor varies depending on the ligand bound. J. Cell. Biochem. 94: 540–553, 2005.

Key words: ribosomal protein S19; antibodies; complement C5a; apoptosis; chemotaxis

Abbreviations used: RP S19, ribosomal protein S19; HA, hemagglutinin peptide-tagged; RT-PCR, reverse transcriptase polymerase chain reaction; *E. coli*, *Escherichia coli*; FBS, fetal bovine serum; P/S, ampicillin/streptomycin; pCAIN, pCAGGS-IRES neomycin resistant vector; NIH-mock, mouse NIH3T3 clone transfected with plain pCAIN; NIH-wild-type, mouse NIH3T3 clone transfected with pCAIN bearing HA-tagged wild-type of RP S19 cDNA; NIH-mutant, mouse NIH3T3 clone transfected with pCAIN bearing HA-tagged Gln137Asn mutant of RP S19 cDNA; Mn II, manganese (II); SDS–PAGE, sodium dodecyl sulfate–polyacrylamide gel electrophoresis; PBS, phosphate-buffered saline; PI, propidium iodide; FACS, fluorescence-activated cell sorting.

Grant sponsor: Ministry of Education, Culture, Sports, Science, and Technology Japan (Grant-in-Aid for Scientific Research); Grant number: 15590350; Grant sponsor: Arthritis Research Campaign; Grant number: M0648.

*Correspondence to: Hiroshi Nishiura, MD, Department of Molecular Pathology, Faculty of Medical and Pharmaceutical Sciences, Kumamoto University, 2-1-1 Honjo, Kumamoto 860-0811, Japan.
E-mail: seino@kaiju.medic.kumamoto-u.ac.jp

Received 31 July 2004; Accepted 13 September 2004
DOI 10.1002/jcb.20318

S19 ribosomal protein (RP S19) is a ribosomal protein that plays a role in the translation of mRNA to protein in the protein-producing machinery. In the past decade, we have discovered and characterized an extra-ribosomal function of RP S19 in apoptosis [Nishiura et al., 1996]. We have reported firstly that RP S19 is homologously cross-linked by a transglutaminase-catalyzed reaction, and released into the extracellular milieu during apoptosis; secondly that the homodimer functions as a monocyte-selective chemoattractant in vitro, and recruits circulating monocytes to the apoptotic lesion in vivo; and thirdly that the recruited monocytes clear the apoptotic cells by phagocytosis and rapidly translocate to regional lymph nodes via lymphatics to present potential non-self antigens derived from the apoptotic cells to T cells [Horino et al., 1998; Shrestha et al., 1999; Nishimura et al., 2001; Shibuya et al., 2001; Shrestha et al., 2003].

Several mutations of the RP S19 gene were found in 25% of patients affected by Diamond-Blackfan anemia, a congenital erythroblastopenia [Draptchinskaia et al., 1999]. All of the patients with RP S19 gene mutations were heterozygotes, suggesting that homozygous abnormality of the *RP S19* gene is embryonic lethal, and that erythropoiesis needs a higher level of functional RP S19 molecules than other cellular systems [Matsson et al., 2004]. Recently, the transcription and translation of the *RP S19* gene were shown to be high at early stages followed by decrement by the terminal stage of erythroid differentiation [Da Costa et al., 2003a]. Furthermore, the number of erythroid colonies was significantly increased when RP S19 cDNA was introduced into $CD34^+$ cells of Diamond-Blackfan anemia patients using a lentiviral vector [Hamaguchi et al., 2003]. Therefore, the high expression level of functional RP S19 molecules clearly contributes to erythrocyte differentiation, although the details remain to be elucidated.

It is becoming clear that an apoptotic mechanism is utilized at the final stage of erythrocyte differentiation, to form enucleate reticulocytes. For instance, the commitment of proapoptotic factor Nix in terminal erythroid maturation has been reported [Aerbajinai et al., 2003], and the embryonic lethality caused by defects of erythropoiesis has been demonstrated in a DNase II knock out mouse which degrades chromosomal DNA during apoptosis [Nagata et al., 2003]. Integration between the essential apoptotic mechanism in erythropoiesis and the RP S19 gene abnormality in Diamond-Blackfan anemia suggests a role for RP S19 in apoptosis, possibly different from the role in phagocytic clearance of apoptotic cells by recruitment of circulating monocytes previously observed.

The RP S19 dimer with monocyte chemoattractant activity was initially observed in extracts of rheumatoid arthritis synovial lesion, where a predominantly monocyte infiltration is seen [Nishiura et al., 1996]. We later observed that the RP S19 dimer attracts monocytes via the C5a receptor [Nishiura et al., 1998], whereas the dimer prohibited the migration of polymorphonuclear leukocytes by antagonizing the C5a receptor [Shibuya et al., 2001]. We then identified sub-molecular regions of RP S19 responsible for the agonistic and antagonistic effects of the dimer [Shrestha et al., 2003]. By this dual effect, the RP S19 dimer reproduces the monocyte-predominant infiltration of rheumatoid arthritis when intradermally injected into guinea pigs.

There are several reports on the presence of apoptotic cells in the rheumatoid arthritis synovial lesion [Baier et al., 2003; Davis, 2003]. The majority of the apoptotic cells seemed to be fibroblastic cells. Recently, a strong C5a receptor gene expression was reported in fibroblastic cells present in the synovial lesion [Neumann et al., 2002], although the role of the C5a receptor on the fibroblastic cells remains unclear. At present, we speculate that the RP S19 dimer could play a role in apoptosis in the rheumatoid arthritis synovial lesion, as suggested for erythropoiesis.

Here we have examined the proposed novel function of the RP S19 dimer in apoptosis using the metal-induced apoptotic model of fibroblasts with NIH3T3 cell line in vitro. Initially, we investigated the effect of replacement of mouse RP S19 in a part with a mutant of human RP S19 that is incapable of dimerization. Finally we defined the RP S19 dimer as a pro-apoptotic ligand that functions by binding to the C5a receptor.

MATERIALS AND METHODS

Materials and Reference Compounds

Restriction enzymes (BamH I, EcoR I, Nde I, EcoR V, Who I, and Sal I), a reverse-transcriptase polymerase reaction (RT-PCR) kit (TAKARA RNA PCR^{TM} Kit (AMV Ver.2.1), T4

DNA polymerase, a DNA ligation kit, *Escherichia coli* (*E. coli*) strains (DH5α and JM109) and isopropyl-β-D-thiogalactopyranoside were purchased from TaKaRa Biomedicals (Otsu, Japan). pBluescript M13 + KS cloning vector was purchased from Stratagene (La Jolla, CA). BigDye® Terminator v1.1 Cycle Sequencing Kit was purchased from Applied Biosystems (Tokyo, Japan). Qiagen Plasmid Midi Kit, RNeasy Mini Kit, and plasmid pQE-30 were purchased from Qiagen K.K. (Tokyo, Japan). SeaKem GTG agarose and NuSieve GTG agarose were purchased from FMC (Rockland, ME). An *E. coli* strain BL21(DE3) and plasmid pET11a were obtained from Novagen, Inc. (Madison, WI). RPMI 1640 medium was purchased from Nissui Pharma. Co. (Tokyo, Japan). Fetal bovine serum (FBS), ampicillin, penicillin/streptomycin (P/S), and Geneticin® were products of Gibco BRL (Paisley, Scotland). Four millimeter gap cuvettes, ϕ 35 and 100 mm cell culture dishes and other goods for cell culture were purchased from Asahi Techno Glass Co. (Tokyo, Japan). A SP-5PW column was obtained from Tosoh Company (Tokyo, Japan). HiTrap Chelating HP and Heparin^{R} columns, ECL Plus Western blotting detection system, and an electrophoresis calibration kit for molecular weight determination of low molecular weight proteins were purchased from Pharmacia (Uppsala, Sweden). Immobilon-P^{SQ} transfer membrane and Amicon® Ultra concentrator with cut off molecular size 5,000 were purchased from Millipore Corporation (Bedford, USA). μMACS hemagglutinin peptide-tagged (HA) protein isolation kit was obtained from Daiichi-Chemicals (Tokyo, Japan). Diisopropyl fluorophosphate, pepstatin A, and *N*-ethylmaleimide were purchased from Peptide Institute (Osaka, Japan). Block Ace^{TM} powder was purchased from Dainihonseiyaku (Okaka, Japan). Sodium deoxycholate was purchased from Difco Laboratory (Detroit, MI). Transglutaminase was obtained from Sigma-Aldrich, Inc. (MO, USA). NMePhe-Lys-Pro-dCha-dCha-dArg, which had been synthesized as described previously [Konteatis et al., 1994], was a kind gift from Prof. N. Nishino of Kyushu Institute of Technology, Kitakyushu, Japan. Recombinant mouse C5a was prepared as described previously. The binding capacity and function of the mouse C5a when analyzed using a cell line transfected with mouse C5a receptor were equivalent to those of the human [Cain et al., 2000]. Unless otherwise specified, all other chemicals were obtained from Wako Pure Chemicals (Osaka, Japan).

Antibodies

Two types of anti-human RP S19 rabbit IgG antibodies were prepared, using recombinant human RP S19 protein, and a keyhole limpet hemocyanin-conjugated synthetic 15mer peptide, Arg-Lys-Leu-Thr-Pro-Gln-Gly-Gln-Arg-Asp-Leu-Asp-Arg-Ile-Cys (RP S19 from Arg121 to Ile134 with a Cys at the C-terminal). An anti-mouse C5a receptor rat IgG2b monoclonal antibody (20/70) was prepared as described previously [Soruri et al., 2003]. Anti-HA rabbit IgG, HRP-conjugated anti-rabbit IgG goat IgG, FITC-conjugated anti-rabbit IgG goat IgG, and FITC-conjugated anti-rat IgG goat IgG were purchased from Santa Cruz (Kumamoto, Japan). A PE-conjugated anti-mouse annexin V monoclonal antibody was purchased from MBL (Nagoya, Japan). Control rat and rabbit IgGs were obtained from Sigma (Kyoto, Japan).

Preparation of HA-Tagged Wild-Type and Gln137Asn Mutant Human RP S19 cDNA

Wild-type and the Gln137Asn mutant human RP S19 cDNAs were prepared as described previously [Nishiura et al., 1999]. To insert HA (YPYDVPDYA) between Gly3 and Val4 of these human proteins, PCR was performed with primer pair HA-RP S19 s1 and HA-RP S19 as1 (Table I). After each cDNA was inserted in the EcoR I and BamH I restriction sites of pBluescript M13 + KS cloning vector, the nucleotide sequence of each PCR product was confirmed by ABI PRISM® 310 (Applied Biosystems) using BigDye Terminator v1.1 Cycle Sequencing Kit with the primer pair T7 and T3 according to the manual of the company.

To check the potential toxicity of HA on the chemoattractant activity of wild-type HA-RP S19 dimer, we prepared the pET 11a vector with wild-type HA-RP S19 cDNA. An Nde I site was made at NH_2-terminal position of wild-type HA-RP S19 cDNA by PCR with primer pairs HA-RP S19 s2 and HA-RP S19 as1 (Table I). PCR product was inserted between Nde I and BamH I sites of pET 11a vector.

Preparation of Over-Expression Vector pCAGGS-IRES Neomycin

Bearing cDNA for wild-type or Gln137-Asn mutant HA-RP S19. pCAGGS-IRES neomycin resistant vector, pCAIN [Fukushima

TABLE I. List of the Synthesized Primer Oligonucleotides

	Sense	Anti-sense
HA-RP S19	s1: cggaattcatgcctggatacccatacg atgttccagattacgctgttactgtaaaagac s2: ggaattccatatgcctggatacccatac	as1: cgggatcctcactaatgctt cttgttggc
CMV	ggtcattagttcatagcccatatatggagt	cgacccatggtaatagctatga
Mouse β-actin	caacggctccggcatgtgc	ctcttgctctgggcctcg
Mouse RP S19	cccggagttactgtaaaagacgttaaccag	ccagcttgactgtgtccacccatt
Human RP S19	tacccatacgatgttccaga	gtagaaccagttctcatcgtag
Mouse C5aR	ttgtgttgcctctgctcact	atcaccactttgagcgtcttgg

HA-RP S19, hemagglutinin peptide-tagged S19 ribosomal protein; CMV, cytomegalovirus promoter; C5aR, C5a receptor.

et al., 1997; Matsuyoshi et al., 2004], was kindly provided by Dr. H. Matsuyoshi of Kumamoto University. The wild-type and Gln137Asn mutant HA-RP S19 cDNAs in pBS were opened at BamH I and Who I sites and made blunt-end sites with T4 DNA polymerase. After cutting off another EcoR I site, above cDNAs were, respectively, inserted to EcoR I and EcoR V sites of pCAIN (see Fig. 1). pCAIN bearing wild-type or Gln137Asn mutant HA-RP S19 cDNA, and plain pCAIN were, respectively, transfected to the competent *E. coli* DH5α cells. Each cDNA was recovered using Qiagen Plasmid Midi Kit and concentrated at a concentration of 1 mg/ml.

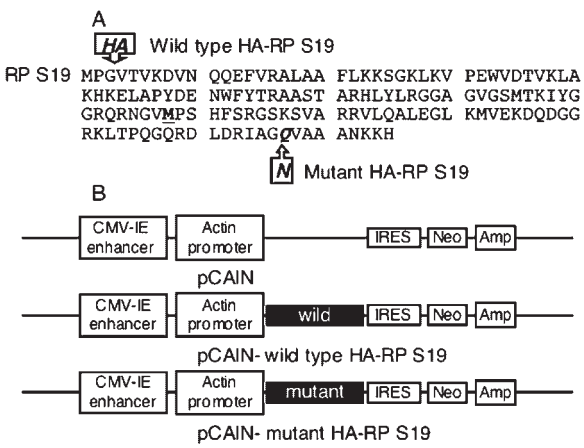

Fig. 1. Constructs of expression vectors bearing human S19 ribosomal protein (RP S19) cDNAs and their product proteins. **A**: Amino acid sequences of the product proteins derived from the constructs. In the human RP S19, a regional sequence of hemagglutinin (HA), YPYDVPDYA, is inserted between Gly3 and Val4. In the mutant HA-RP S19, Gln137, which is an essential residue to form the cross-linked dimer by a transglutaminase-catalyzed reaction, is mutated to Asn. Only one amino acid residue differs between the human and mouse molecules; Met88 (M) in the human is Arg88 in the mouse. **B**: Constructs of the expression vector (pCAGGS-IRES-Neo, pCAIN) and the vectors bearing HA-RP S19 cDNA or its Gln137Asn mutant.

Establishment of Mouse NIH3T3 Clones Transformed With pCAIN

Bearing wild-type or Gln137Asn mutant HA-RP S19 cDNA. Mouse NIH3T3 cells were maintained in RPMI 1640 medium containing non-heat-inactivated 10% FBS and 100 μg/ml P/S. After being harvested, they were suspended in RPMI 1640 medium at a density of 2.5×10^7 cells/ml and subjected to electroporation in a Gene Pulsar II (Nippon Bio-Rad Laboratories, Tokyo, Japan) in a 4 mm gap cuvette using 200 V and 950 μF, in the presence of 40 μg of linearized plasmid DNA. Twenty four stable transfected clones were obtained by the serial dilution method in 250 μM of Geneticin, and successful transfection confirmed by genomic PCR targeting the human cytomegalovirus promoter in pCAIN with a suitable primer pair (Table I). We then selected the best clone for each transformant with regard to the growth rate of the cloned cells. They were named NIH-mock ((mouse NIH3T3 clone transfected with plain pCAIN) pCAIN alone), NIH-wild-type ((mouse NIH3T3 clone transfected with pCAIN bearing HA-tagged wild-type of RP S19 cDNA) pCAIN bearing wild-type HA-RP S19 cDNA), and NIH-mutant ((mouse NIH3T3 clone transfected with pCAIN bearing HA-tagged Gln137Asn mutant of RP S19 cDNA) pCAIN bearing Gln137Asn mutant HA-RP S19 cDNA), respectively.

Induction of Apoptosis With Manganese (II) (Mn II) in NIH3T3 Clones

Apoptosis of the NIH3T3 clones was induced with Mn II according to the method of Oubrahim et al. [2002]. In brief, after culturing 1.5×10^5 cells/ml of the NIH3T3 clones for 48 h in a ϕ 35 mm cell culture dish, the medium was changed to fresh medium containing 0.25 mM $MnCl_2$. After further incubation for 24 or 48 h,

apoptotic cells were visualized by staining with Hoechst 33342 and Giemsa solution. As a control, necrosis was induced in the same cells with 1 mM H_2O_2 [Ricart and Fiszman, 2001]. The ratio of dead cells was calculated by the following formula: % dead cells = (number of trypan-blue positive cells in the culture supernatant and on the culture dish/total number of cells in the culture supernatant and on the culture dish) × 100.

RT-PCR

After recovering the NIH3T3 clonal transfectants, the mRNA fraction was prepared using the RNeasy Mini kit, and the transcription levels of particular genes analyzed by RT-PCR using the Takara RNA PCR^{TM} kit (AMV) Ver.2.1 with specific primer pairs (Table I) according to the instruction manual. RT-PCR was performed under following conditions: temperatures and time periods of the denature, the annealing, and the elongation were 94, 62, and 72°C, respectively, all for 30 s. The elongation cycle was 30 cycles. The level of transcription was determined using NIH Image 1.63 image analysis software, according to a following formula: relative transcription rate of sample gene to actin gene = (density of sample band/density of β-actin band) × 100%.

Sodium Dodecyl Sulfate–Polyacrylamide Gel Electrophoresis (SDS–PAGE)

Electrophoresis was performed using 15% polyacrylamide gels according to the method of Laemmli [1970]. The NIH-wild-type and NIH-mutant clones were cultured in ϕ 100 mm culture dishes, and treated with 0.25 mM $MnCl_2$. After 30 h, each culture supernatant and cells were separately collected. The supernatants were immediately treated with a protease inhibitor cocktail (1 mM diisopropyl fluorophosphate, 4 mM EDTA, 0.01 mM *N*-ethylmaleimide, and 0.01 mM pepstatin A, at the final concentrations), then concentrated 1,000-fold using Amicon Ultra concentrators, cut off molecular size 5,000. The cells were washed twice in PBS and extracted for 30 min at 4°C with the lysis buffer attached to the kit described bellow. After centrifugation at 12,000 rpm for 20 min at 4°C, HA-RP S19-related molecules in the cells and supernatants were collected using anti-HA antibody-coupled μMACS microbeads and the magnetic μMACS bead separator. Samples were boiled for 2 min in the presence of SDS, and applied to the SDS–PAGE. The gel was stained with Coomassie blue.

Western-Blotting Analysis

Initially, samples containing HA-labeled proteins were subjected to SDS–PAGE, then transferred to Immobilon-P^{SQ} membranes using a semi-dry blotting machine, AE-6677 (Atto, Tokyo, Japan). After washing twice in PBS, the membrane was treated with 1% Block Ace for 1 h at 22°C with continuously shaking, then reacted with the anti-RP S19 peptide rabbit IgG antibodies for 2 h at 22°C. After another incubation with HRP-conjugated anti-rabbit IgG goat IgG for 1 h at 22°C, the bound HRP was detected using the ECL Plus Western blotting detection system.

Fluorescent Immuno-Cytochemistry

After washing twice in PBS, NIH3T3 clonal cells were fixed in 1% (w/v) paraformaldehyde for 10 min, then treated with 1% Block Ace at 22°C for 1 h. For the detection of intracellular RP-S19, the cells were treated with 0.1% of Triton X-100 for 30 min. For immuno-cytochemical detection, the cells were initially treated with the anti-HA rabbit IgG antibodies, the anti-mouse C5a receptor rat IgG2b monoclonal antibody (20/70) or the PE-conjugated anti-mouse annexin V monoclonal antibody for 2 h at 22°C. In the former two cases, cells were treated further with FITC-conjugated anti-rabbit IgG goat IgG or FITC-conjugated anti-rat IgG goat IgG for 1 h at 22°C. In some experiments, cell nuclei were stained with propidium iodide (PI). Fluorescence was observed using an Olympus Fluoroview FV500 (Olympus, Tokyo, Japan).

Fluorescence-Activated Cell Sorting (FACS) Analysis

NIH3T3 transfectants were suspended in 500 μl of PBS containing 5% FBS (FACS medium) at a density of 1×10^5 cells/ml, and incubated with normal rat IgG for 20 min at 4°C to block non-specific IgG binding. For analysis of the C5a receptor, cells were incubated with 5 μg/ml of anti-mouse C5a receptor rat IgG monoclonal antibody (20/70) for 30 min at 4°C, and with FITC-conjugated anti-rat IgG goat IgG. For the analysis of phosphatidylserine exposure, cells were incubated with PE-conjugated anti-mouse annexin V monoclonal antibody for 30 min at 4°C. Cell nuclei was

stained with 7-aminoactinomycin. FACS was performed with a FACS Caliber (BD, Tokyo, Japan).

Statistical Analysis

Student's *t*-test (two-tailed test) was used to evaluate statistical significance.

RESULTS

Establishment of RP S19-Transfected NIH3T3 Cell Lines

Three stable clonal cell lines, transfected with pCAIN plasmid bearing wild-type HA-RP S19 cDNA (NIH-wild-type), HA-RP S19 Gln137Asn mutant (NIH-mutant) or with pCAIN plasmid alone (NIH-mock), respectively, were established. The primary structures of the RP S19 proteins, and the designs of the plasmid constructs, are shown in Figure 1A,B.

The growth rates of these clones were examined to eliminate the possibility of undesired effects of transfection on basic cell physiology. All clones grew on ϕ 35 mm culture dishes forming adherent colonies (see Fig. 3). As shown in Figure 2A, there was almost no difference between the growth rates of the clones after seeding at 5×10^4 cells/dish. Because the viability was almost 100% until at least the 80% confluent stage (data not shown) obtained 48 h after seeding, we used the clones at the 80% confluent stage in the following experiments.

The intensities of expression of transfected wild-type and mutant *HA-RP S19* genes and the

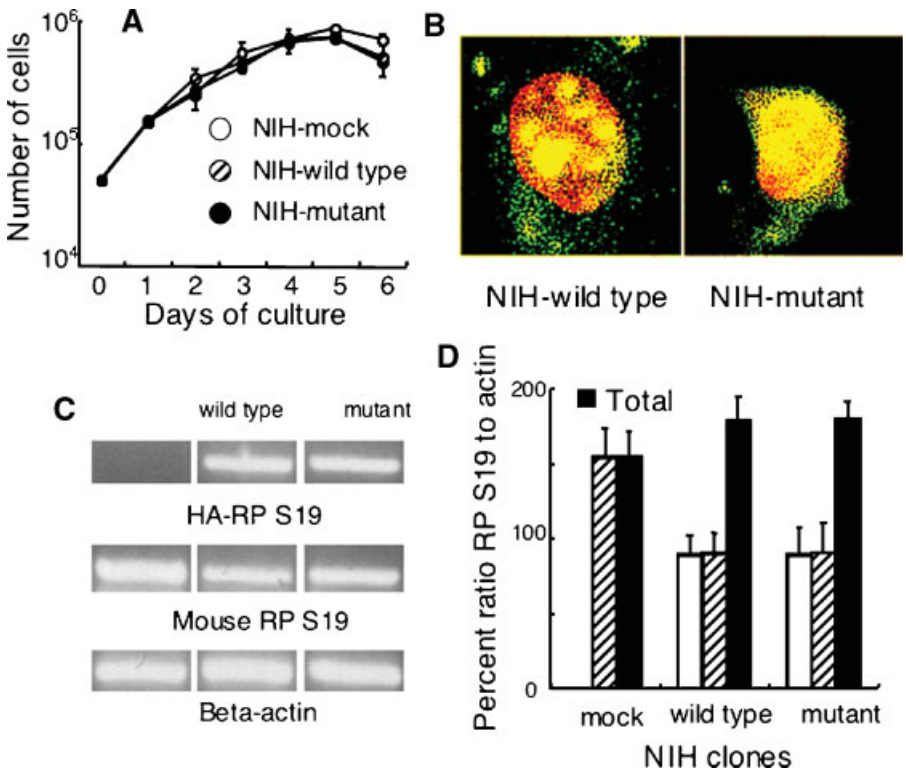

Fig. 2. Expression of RP S19-related genes in transformed clones. **A**: 5×10^4 cells were seeded in a ϕ 35 mm plastic dish, and cultured at 37°C under 5% CO_2 (see Materials and Methods). The number of cells was counted every day by the trypan-blue dye exclusion method. The open, slashed, and closed circles denote NIH-mock, NIH-wild-type, and NIH-mutant, respectively. **B**: Immunocytochemical observation of the transfected gene-derived proteins in transformant clones, NIH-wild-type and NIH-mutant. The cells grown on slide glasses were fixed with 1% paraformaldehyde, treated with 0.1% Triton X-100, and reacted with anti-HA rabbit IgG and with FITC-conjugated anti-rabbit IgG goat IgG, in this order. After the cell nucleus was stained with PI, the cells were observed by a confocal laser-scanning microscope (CLSM). Magnification is ×60. **C**: A semi-quantitative RT-PCR analysis was performed for the host RP S19 mRNA, for the transfected wild-type and mutant type HA-RP S19 mRNAs, and for β-actin using a specific primer pair for each mRNA as listed in Table I. The **left**, **center**, and **right lanes** are NIH-mock, NIH-wild-type, and NIH-mutant clones, respectively. **D**: The intensities of the gel bands were measured using an image analyzer with NIH Image 1.63 software. The open, slashed, and closed columns denote the relative transcription level to the actin gene of the transfected *HA-RP S19* genes, the host *RP S19* gene, and their sum, respectively. Values are mean ± SD (three separate experiments with triplicate samples were performed).

endogenous mouse *RP S19* gene were examined by RT-PCR. As shown in Figure 2C,D, the typical expression intensity of the mouse *RP S19* gene in NIH-mock was 154.25 ± 16.5. In the other clones, the expression intensities of the mouse *RP S19* gene decreased to about a half of that of NIH-mock (NIH-wild-type; 90.14 ± 13.53 and NIH-mutant; 90.36 ± 19.58), and the transfected genes expressed at levels similar to those of the mouse gene (NIH-wild-type; 88.87 ± 12.92 and NIH-mutant; 89.26 ± 17.73).

The localization of wild-type or mutant HA-RP S19 proteins, observed by fluorescent immunocytochemistry using anti-HA antibodies, was predominantly in the nucleus (Fig. 2B). The distribution pattern was similar to that of intrinsic RP S19 as reported by Da Costa et al. [2003b]. Therefore, the expression levels of the *RP S19* genes in total were not different among the transfected clones and untransfected cells, and exogenous wild-type and mutant HA-RP S19 proteins should be working normally in the ribosome.

Effects of Transfection With Human RP S19 on Mn II-Induced Apoptosis

Apoptosis was induced in the cultured clones by changing the culture medium to one containing 0.25 mM $MnCl_2$. To morphologically distinguish apoptosis from necrosis, some culture dishes were treated with medium containing 1 mM H_2O_2 instead of $MnCl_2$, to induce necrosis. As apoptosis progressed, shrinkage of cell body and nucleus with chromatin condensation were observed (Fig. 3A), before the apoptotic cells finally detached from the dish surface. The shrunken nuclei with condensed chromatin were strongly stained by Hoechst 33342 dye (data not shown). These morphological characteristics differed from those of necrotic cells which had swollen cell bodies and nuclei (Fig. 3A), indicating the occurrence of apoptosis as reported by Oubrahim et al. [2002]. We quantified the intensity of apoptosis (including the detached cells), according to the formula described in Materials and Methods, at 24 and 48 h after Mn II loading. Commonly, after 24 h the percentage of dead cells was below 20%, whereas after 48 h, it dramatically increased up to 90%.

As shown in Figure 3B, NIH-mutant acquired resistance to the induction of apoptosis by Mn II (64.7 ± 8.8). In contrast, NIH-wild-type had a slightly higher sensitivity (92.9 ± 7.2) than that of NIH-mock (86.6 ± 1.3) to the induction of apoptosis. These results suggested the participation of the cross-linked homodimer of RP S19 in metal-induced apoptosis of NIH3T3 cells.

Release of RP S19 Dimer During Apoptosis

In previous studies using human cell lines such as HL-60 and AsPC-1, we observed the extracellular release of the monocyte chemotactic RP S19 dimer during heat-induced apoptosis. In the current study, we have examined the release of the RP S19 dimer in metal-induced

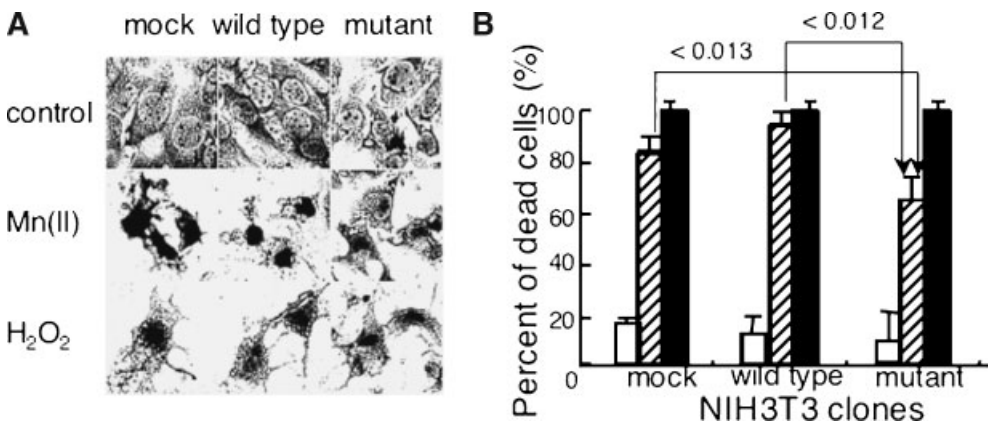

Fig. 3. Acquired resistance of NIH3T3 cells against manganese (II) (Mn II)-induced apoptosis by transformation with HA-RP S19 Gln137Asn mutant cDNA. **A**: At 80% confluence stage, apoptosis, or necrosis was induced with 0.25 mM $MnCl_2$ or with 1 mM of H_2O_2, respectively. At 48 h after the reagent loading, cells were fixed and stained with Giemsa. **Left**, **center**, and **right lanes** are NIH-mock, NIH-wild-type, and NIH-mutant, respectively. Magnification is ×100. **B**: At 48 h after the reagent loading, total cells including detached ones were harvested, and the ratio of dead cells was measured by the trypan-blue dye exclusion method. The open, slashed, and black columns denote percent of dead cells in the control, Mn II-loaded, and H_2O_2-loaded dished, respectively. Values are mean ± SD (three separate experiments with triplicate samples were performed).

apoptosis of NIH-wild-type or NIH-mutant by means of Western blot analysis using anti-RP S19 antibodies. As shown in Figure 4A, immunopositive bands corresponding to the HA-RP S19 dimer were observed in the culture supernatant of the metal-induced apoptotic NIH-wild-type. In contrast, no band corresponding to the dimer was seen in NIH-mutant cells. We also observed an up-regulation of mouse type 2 transglutaminase during Mn II-induced apoptosis in NIH-wild-type and NIH-mock, but not in NIH-mutant, as determined by RT-PCR (data not shown).

Inhibition of Apoptosis With Anti-RP S19 Antibodies in Transfected NIH3T3 Cells

In previous studies, we investigated the monocyte chemoattractant activity of the RP S19 dimer released into the apoptotic cell culture supernatant. However, the results obtained in this report suggest a pro-apoptotic effect of the RP S19 dimer in Mn II-induced apoptosis. Therefore, we examined whether anti-RP S19 antibodies could prevent metal-induced apoptosis of transfected NIH3T3 cell lines. As shown in Figure 4B,C, the presence of anti-RP S19 antibodies during the Mn II treatment reduced the rates of apoptosis of all of the clones to around 40% (NIH-mock: 42.6 ± 4.7, NIH-wild-type: 47.6 ± 5.2, and NIH-mutant: 38.3 ± 8.3). In contrast to this, normal rabbit IgG did not significantly affect the apoptosis rates of the cell lines (NIH-mock: 79.7 ± 8.9, NIH-wild-type: 95.9 ± 4.9, and NIH-mutant; 59.6 ± 4.0).

Overcoming the Inhibition of Apoptosis by Addition of Extracellular RP S19 Dimer

Because the experimental results with anti-RP S19 antibodies strongly suggested that the RP S19 dimer promoted or augmented the metal-induced apoptosis by an autocrine mechanism, we examined whether an extracellular supplement of human RP S19 dimer could reproduce the augmentation of apoptosis in the clone transformed with the Gln137Asn RP S19 mutant gene. As shown in Figure 4E, supplementation with RP S19 dimer enhanced the cell-death ratio of transfected NIH3T3 cells up to almost 100% (NIH-mock: 96.2 ± 2.9, NIH-wild-type: 97.8 ± 0.91, and NIH-mutant: 94.5 ± 3.8), whereas the treatment with RP S19 monomer had no effect (data not shown). The augmented cell-death was confirmed to be due to apoptosis by the morphologic characteristics (Fig. 4D) and by staining with Hoechst 33342 dye (data not shown). The addition of RP S19 dimer to the cells in the absence of Mn II treatment had no effect at all. These results indicate that the presence of an RP S19 dimer-mediated augmentation mechanism in Mn II-induced apoptosis in NIH3T3 fibroblasts.

Increased Cell Surface Expression of C5a Receptor During Apoptosis of Transfected NIH3T3 Cells

Leukocyte chemotaxis is a receptor-mediated event, and the receptor on monocytes for the chemoattractant RP S19 dimer is the C5a receptor. We, therefore, examined whether the pro-apoptotic effect of the RP S19 dimer on NIH3T3 fibroblasts was also a C5a receptor-mediated event. Because the C5a receptor is usually thought to be a leukocyte receptor, we initially determined whether the C5a receptor was present on the surface of NIH3T3 cells by means of FACS. As shown in Figure 5A, C5a receptor was detectable on the surface of only $1.8 \pm 0.5\%$ of the total cultured cells. We, therefore, next examined whether the C5a receptor on the NIH3T3 cell surface was up-regulated during metal-induced apoptosis. As shown in Figure 5A, the C5a receptor-positive cell ratio increased at 24 h after the induction of apoptosis with Mn II. The increment of the positive cell ratio was more significant in NIH-wild-type (11.2 ± 1.0) than those of the NIH-mutant (3.3 ± 0.1) and NIH-mock (4.0 ± 0.6), respectively. The increase in the C5a receptor-positive cell population correlated with that of phosphatidylserine-positive one (NIH-wild-type; 12.2 ± 0.6), which was visualized with fluorescent-labeled annexin V. The majority of the positive cells were double positive for the C5a receptor and cell surface phosphatidylserine (Fig. 5B).

To examine whether the increased cell surface expression of the C5a receptor was due to de novo synthesis, we measured levels of C5a receptor mRNA by means of RT-PCR. As shown in Figure 5C,D, C5a receptor mRNA was constitutively expressed in all of the clones at low levels (ratio of C5a receptor mRNA to actin mRNA: NIH-mock: 29.3 ± 1.6, NIH-wild-type: 30.2 ± 1.6, and NIH-mutant: 25.0 ± 1.4). C5a receptor mRNA levels were significantly enhanced after 8 h of Mn II treatment (NIH-mock: 52.1 ± 2.8, NIH-wild-type: 55.7 ± 3.0, and NIH-mutant: 66.9 ± 3.6).

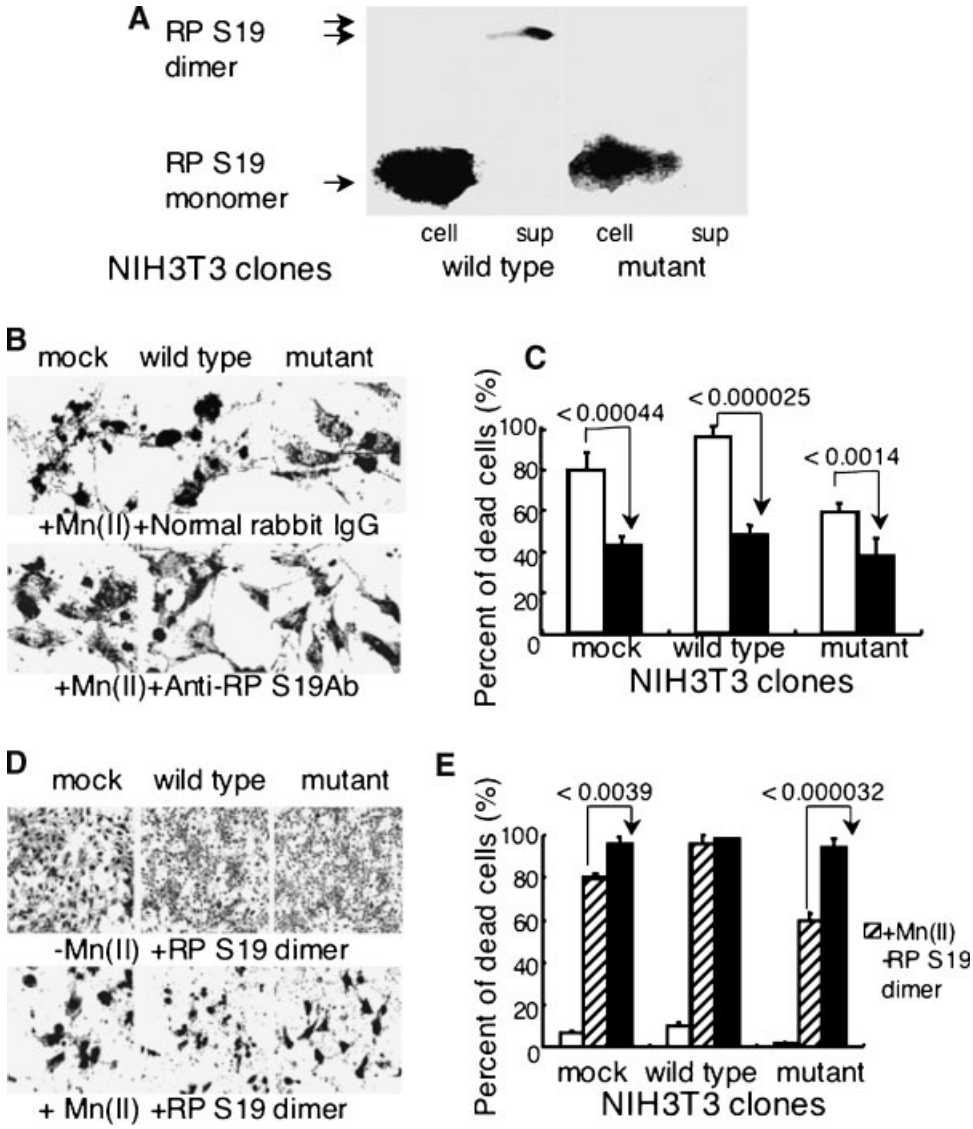

Fig. 4. Augmentation of Mn II-induced apoptosis by extracellular supplement of RP S19 dimer. **A**: The NIH-wild-type and NIH-mutant clones were treated with 0.25 mM $MnCl_2$. After 30 h, each culture supernatant and cells were separately collected. The supernatants were immediately treated with a protease inhibitor cocktail, then concentrated. The cells were extracted with a lyses buffer for 30 min at 4°C. After centrifugation, HA-RP S19-related molecules in the supernatants were collected using anti-HA antibody-coupled μMACS microbeads and the magnetic bead separator, and were eluted from the beads. Samples were subjected to Western blot analysis using anti-RP S19 peptide rabbit IgG as the first antibody (see Materials and Methods). The single and double arrows denote electrophoretic positions of the HA-RP S19 monomer (molecular weight of 18 kDa) and the HA-RP S19 dimer (36 kDa), respectively. **B**: Three transformant clones were treated with 0.25 mM $MnCl_2$ for 48 h in the presence of 50 μg/ml of normal rabbit IgG or anti-RP S19 rabbit IgG, respectively. The cells on aliquot dishes were fixed and stained with Giemsa. The **left**, **center**, and **right lanes** are NIH-mock, NIH-wild-type, and NIH-mutant, respectively. Magnification is ×100. **C**: At 48 h, total cells including detached ones in other aliquot dishes were collected, and the ratio of dead cells was measured by the trypan-blue dye exclusion method. The open and closed columns denote the normal rabbit IgG and anti-RP S19 rabbit IgG groups, respectively. Values are mean ± SD (three separate experiments with triplicate samples were performed). **D**: The transformed clones were treated with or without 0.25 mM $MnCl_2$ in the presence or absence of 1×10^{-8} M of recombinant RP S19 dimer for 48 h, respectively. The cells on aliquot dishes were fixed and stained with Giemsa. The **left**, **center**, and **right lanes** are NIH-mock, NIH-wild-type, and NIH-mutant, respectively. Magnification is ×100. **E**: At 48 h, the total cells including detached ones in other aliquot dishes were collected, and the ratio of dead cells was measured by the trypan-blue method. The open, slashed, and closed columns denote the cases incubated in the presence of the RP S19 dimer without $MnCl_2$, the cases treated with $MnCl_2$ in the absence of the RP S19 dimer, the cases treated with $MnCl_2$ in the presence of the RP S19 dimer, respectively. Values are mean ± SD (three separate experiments with triplicate samples were performed).

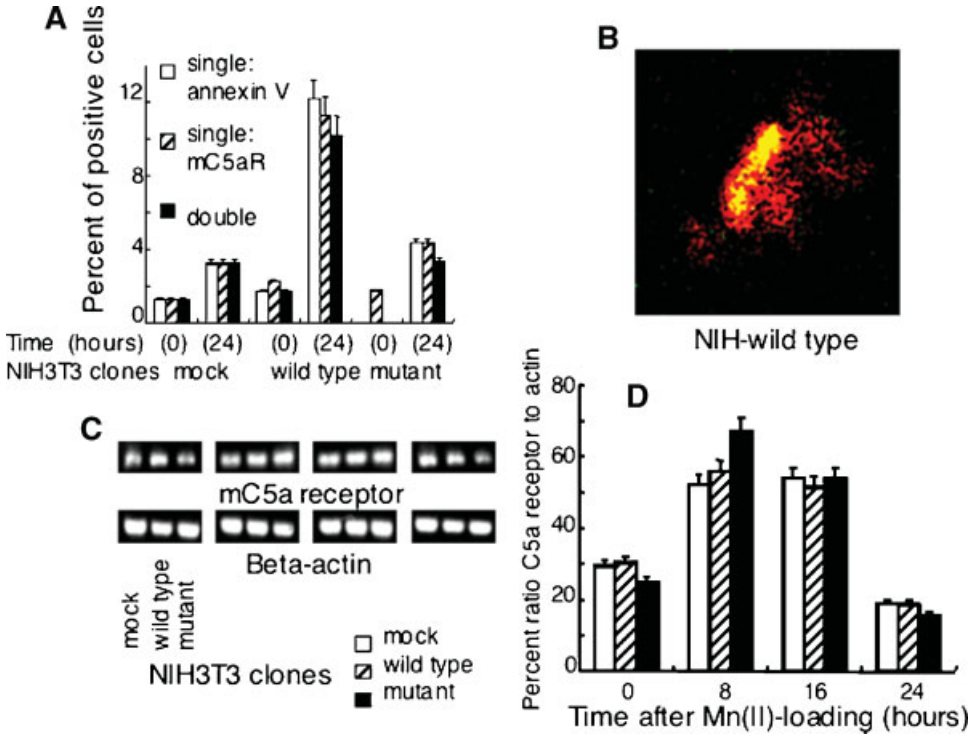

Fig. 5. Emergence of C5a receptor and phosphatidylserine on cell surface during Mn II-induced apoptosis. The clonal cells were incubated in the presence or absence of 0.25 mM $MnCl_2$. At 24 h, the cells were harvested. **A**: Aliquots of the cell samples were stained simultaneously with PE-conjugated anti-annexin V antibodies and with FITC-conjugated anti-mouse C5a receptor rat IgG monoclonal antibody (20/70). After the cellular nucleus was stained with 7AAD, cells were analyzed by fluorescence-activated cell sorting. The open, slashed, and closed columns denote the percentage of annexin V-positive, mouse C5a receptor-positive, and double-positive cells, respectively. Values are mean ± SD (three separate experiments with triplicate samples were performed). **B**: Aliquots of the cultured cells were fixed and stained with the same antibodies as used in (A), and observed using the CLSM. Only NIH-wild-type cells are shown. Magnification is ×60. **C**: The clonal cells were cultured in the presence of 0.25 mM $MnCl_2$. At denoted time points after Mn II-loading, the mRNA fractions of cell aliquots were prepared, and the semi-quantitative RT-PCR analysis was performed for the C5a receptor using a specific primer pair as listed in Table I. The **left**, **center**, and **right lanes** of each photo picture are NIH-mock, NIH-wild-type and NIH-mutant clones, respectively. **D**: The intensities of the gel bands were measured as Figure 2. The open, hatched, and closed columns denote the relative transcription level to the actin gene of the *C5a* gene in NIH-mock, NIH-wild-type, and NIH-mutant, respectively. Values are mean ± SD (three separate experiments with triplicate samples were performed).

Inhibition of Apoptosis With Anti-C5a Receptor Monoclonal Antibody or With C5a Receptor Antagonist in Transfected NIH3T3 Cells

To examine whether C5a receptor on NIH3T3 cells participated in the RP S19 dimer-mediated augmentation of metal-induced apoptosis, we first used an anti-mouse C5a receptor monoclonal antibody. As shown in Figure 6A,B, the presence of anti-C5a receptor antibody reduced the apoptotic ratio down to 40% in all clones (NIH-mock: 38.9 ± 5.7, NIH-wild-type: 42.8 ± 5.2, and NIH-mutant: 34.0 ± 6.2). This maximal reduction rate was not changed by the simultaneous presence of anti-RP S19 antibodies with the anti-C5a receptor antibody (data not shown).

To confirm the participation of C5a receptor in the pro-apoptotic effect of RP S19 dimer, we used a C5a receptor antagonist. As shown in Figure 6C,D, the presence of the C5a receptor antagonist also reduced the metal-induced apoptosis rate down to about 40% (NIH-mock: 24.6 ± 2.4, NIH-wild-type: 38.6 ± 2.2, and NIH-mutant: 32.3 ± 2.3).

Effect of C5a on Mn II-Induced Apoptosis in NIH3T3 Cells

The C5a receptor has two intrinsic ligands, namely the RP S19 dimer and C5a/C5a desArg. We examined the effect of C5a on Mn II-induced apoptosis using the recombinant mouse C5a. In contrast to the RP S19 dimer, C5a inhibited apoptosis (Fig. 7). The addition of a final

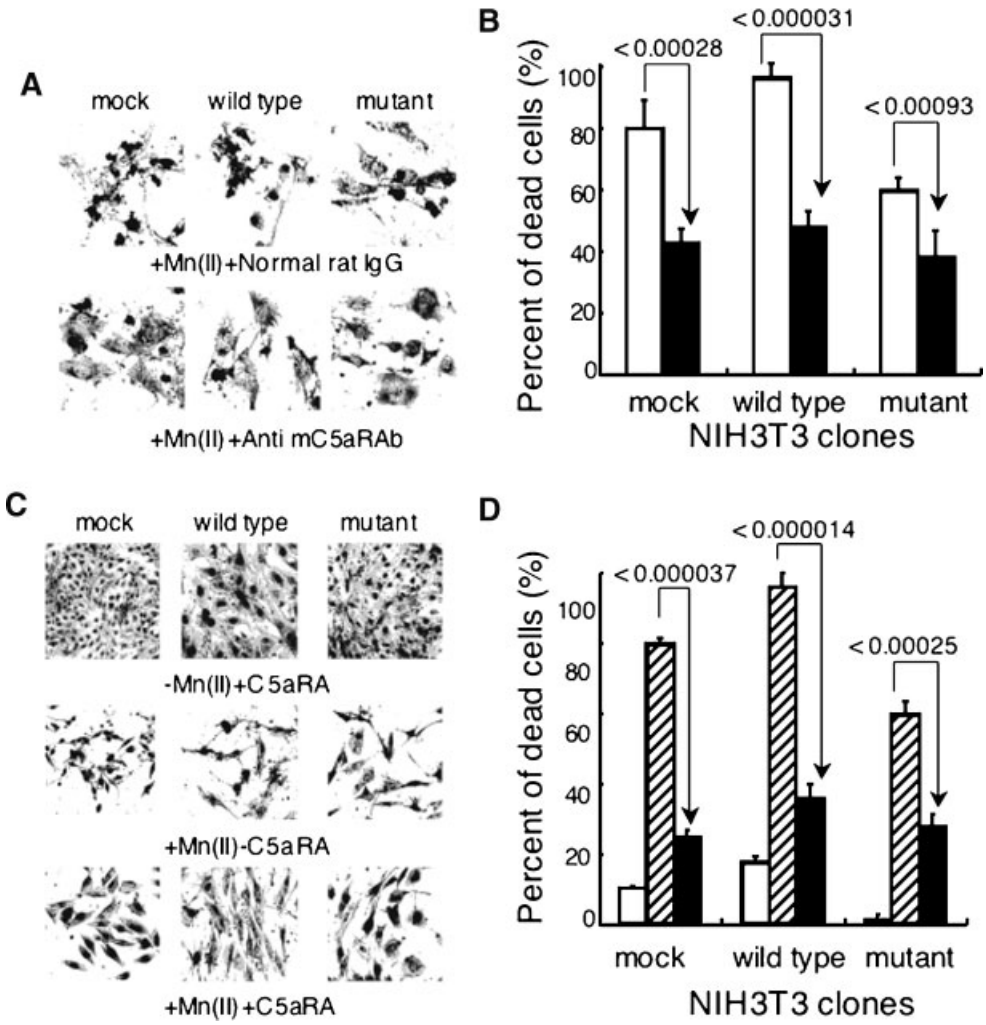

Fig. 6. Inhibition of Mn II-induced apoptosis by anti-C5a receptor antibody and C5a receptor antagonist. The clonal cells were cultured in the simultaneous presence of 0.25 mM $MnCl_2$ and 50 μg/ml of anti-mouse C5aR rat monoclonal antibody (20/70) or of normal rat IgG for 48 h, respectively. **A**: The cells on aliquot dishes were fixed and stained with Giemsa. The **left**, **center**, and **light lanes** are NIH-mock, NIH-wild-type, and NIH-mutant, respectively. The magnification is ×100. **B**: The total cells including detached ones in other aliquot dishes were, respectively, collected, and the ratio of dead cells was counted by the trypan-blue method. The open and closed columns denote the cell samples cultured with the normal rat IgG and with the anti-C5a receptor antibody, respectively. Values are mean ± SD (three separate experiments with triplicate samples were performed). **C**: The clonal cells were, respectively, cultured for 48 h in three different conditions; in the presence of 10^{-6} M C5a receptor antagonist (NMePhe-Lys-Pro-dCha-dCha-dArg), in the presence of 0.25 mM $MnCl_2$, and the simultaneous of the antagonist and $MnCl_2$. The cells on aliquot dishes were fixed and stained with Giemsa. The **left**, **center**, and **right lanes** are NIH-mock, NIH-wild-type, and NIH-mutant, respectively. The magnification is ×100. **D**: The total cells including detached ones in other aliquot dishes were, respectively, collected, and the ratio of dead cells was counted by the trypan blue method. The open, slashed, and closed columns denote the cell samples cultured with the antagonist, with $MnCl_2$, and together with the antagonist and $MnCl_2$, respectively. Values are mean ± SD (three separate experiments with triplicate samples were performed).

concentration of 10^{-6} M C5a reduced the cell-death ratio of all of the clones down to about 45% (NIH-mock: 45.7 ± 3.7, NIH-wild-type: 49.4 ± 3.9, and NIH-mutant: 43.5 ± 7.8). The protection against Mn II-induced cell-death was confirmed to be due to apoptosis by the morphologic characteristics (Fig. 7A). These results indicate the presence of a C5a-mediated protection mechanism in Mn II-induced apoptosis in NIH3T3 fibroblasts.

DISCUSSION

The current study has revealed the pro-apoptotic function of cross-linked homo-dimers or oligomers of RP S19 in Mn II-induced

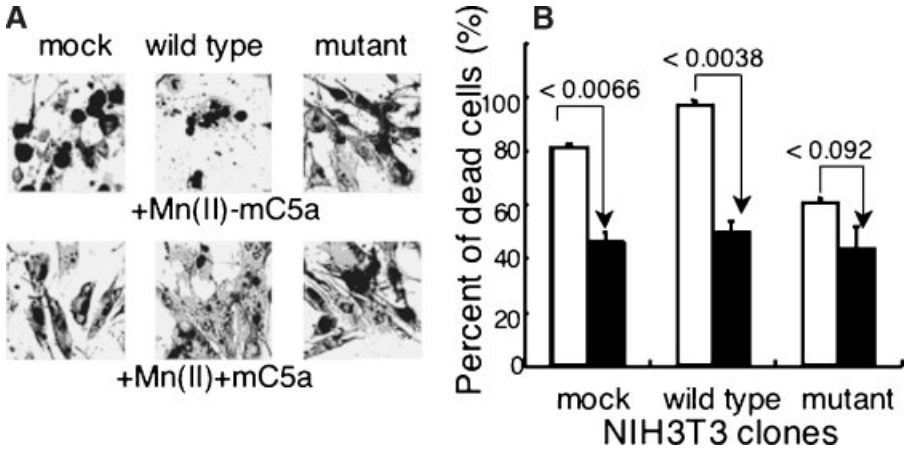

Fig. 7. Effect of C5a on Mn II-induced apoptosis. The clonal cells were treated with 0.25 mM $MnCl_2$ in the simultaneous presence or absence of 10^{-6} M mouse C5a for 48 h, respectively. **A**: The cells on aliquot dishes were fixed and stained with Giemsa. The **left**, **center**, and **right lanes** are NIH-mock, NIH-wild-type, and NIH-mutant, respectively. The magnification is ×100. **B**: The total cells including detached ones in other aliquot dishes were, respectively, collected, and the ratio of dead cells was counted by the trypan-blue method. The open and closed columns denote the cell samples cultured without or with C5a, respectively. Values are mean ± SD (two separate experiments with triplicate samples were performed).

apoptosis of NIH3T3 cells. This has been demonstrated by (1) the reduction of the sensitivity of NIH3T3 cells to the metal-induced apoptosis by the replacement of one monomer of RP S19 with its Gln137Asn mutant (Fig. 3) which is not capable of being cross-linked by the transglutaminase-catalyzed reaction [Nishiura et al., 1998]; (2) the inhibition of this reduction by the addition of RP S19 dimer to the medium (Fig. 4); and (3) the reduction of the apoptosis rate down to about 40% by the presence of anti-RP S19 rabbit IgG (Fig. 4). In metal-induced apoptosis, the RP S19 dimer is formed and released by the apoptotic cells (Fig. 4), and it promotes further apoptosis in an autocrine fashion. To the best of our knowledge, this is the first report on a pro-apoptotic function of a ribosomal component.

In the present study, we used human RP S19 and its antibodies on mouse fibroblastic cells. In the case of RP S19, we do not have to worry about the species difference because the amino acid sequence of this molecule is highly conserved among mammalian species. Only one amino acid residue differs between human and mouse or rat molecules (Met88 in human is Arg88 in the mouse and the rat); similarly, there is no difference between human and guinea pig molecules [Umeda et al., 2004].

In a separate study, we have demonstrated the participation of the RP S19 dimer in the clearance of apoptotic cells by macrophages. In this case, the RP S19 dimer released by the apoptotic cells recruits circulating monocytes in a paracrine fashion. We propose that the RP S19 dimer, therefore, has two different roles in the apoptotic process.

Our study has also revealed that the pro-apoptotic effect of the RP S19 dimer is mediated by the C5a receptor. This has been demonstrated by: (1) treatment with the anti-mouse C5a receptor monoclonal antibody or with the C5a receptor antagonist (Fig. 6) causes the reduction of metal-induced apoptosis to 40%; (2) by the increased expression of the C5a receptor on the cell surface concomitant with the surface exposure of phosphatidylserine during apoptosis (Fig. 5).

Interestingly, the C5a receptor-mediated augmentation of metal-induced apoptosis was not reproduced by C5a itself. In fact, C5a inhibited this apoptosis (Fig. 7), probably due to a competition with the RP S19 dimer for C5a receptor occupation.

The induction of neuronal cell death in vitro was reported by Farkas et al. [1998]. In their experiments, TGW human neuroblastoma cells, which bear a C5a receptor, were exposed to an oligomeric form of a C5a fragment (amino acids: 37–53) peptide. Although the ligand used in their experiments was an artificial oligomeric peptide, DNA fragmentation of the exposed cells was clearly demonstrated morphologically using TdT-mediated dUTP-biotin nick

end-labeling method. Taken together with the results presented in this paper, this indicates that the C5a receptor could play a role in the promotion of apoptosis under some circumstances, even though the C5a receptor does not have the death domain expressed by the pro-apoptotic receptors such as the tumor necrosis factor receptor. More recently, Farkas et al. [2003] have demonstrated the C5a receptor-mediated apoptosis of rat cortical pyramidal neurons. They emphasized the participation of the C5a receptor-mediated neurodegeneration in Alzheimer's disease, because the C5a receptor was detected on human pyramidal cells of the hippocampus and cortex and granular cells of the hippocampus, and the receptor was not detected in cases of Alzheimer's disease. RP S19 dimer is a candidate for the apoptotic ligand for the neuronal C5a receptor, because apoptosis could not be induced when C5a was used instead of the oligomeric C5a fragment peptide. As in our present study, C5a did not induce apoptosis when binding to the C5a receptor.

In our current study, the C5a receptor mRNA was found to be constitutively expressed only at a low level in NIH3T3 fibroblastic cells, but was enhanced by Mn II treatment. On the other hand, fibroblasts that expressed the C5a receptor at high levels on their surface have been demonstrated in the rheumatoid arthritis synovial lesion [Neumann et al., 2002]. Because the RP S19 dimer is present in the synovial lesion, it is likely that C5a receptor-mediated apoptosis of fibroblasts occurs in the synovial lesion.

In the present study, we have demonstrated that the RP S19 dimer-C5a receptor system doubled the Mn II-induced apoptosis rate. The basic apoptotic mechanism appears independent to the augmentation system in Mn II-induced apoptosis. Oubrahim et al. [2002] have recently reported on the intracellular executing mechanism of Mn II-induced apoptosis in NIH3T3 cells. They emphasized that the mechanism was non-mitochondria-mediated but was m-calpain-mediated at least in part: Mn II replaces calcium (II) in the activation of m-calpain, which in turn activates caspase-12 and degrades Bcl-xL, and caspase-3 is finally activated by activated caspase-12. Because they did not notice the augmentation mechanism presently shown at that time, we do not know whether their proposed mechanism is operational in the Mn II-induced apoptosis of NIH3T3 cells.

ACKNOWLEDGMENTS

We thank for members of Department of Molecular Pathology, Kumamoto University; Miss T. Matsuda for the technical assistance with cell culture, and Dr. K. Tokita for his advice on the work with the confocal laser microscope. We also thank Dr. Y. Fukushima of Tokyo University for his kind advice on the usage of pCAIN vector.

REFERENCES

Aerbajinai W, Giattina M, Lee YT, Raffeld M, Miller JL. 2003. The proapoptotic factor Nix is coexpressed with Bcl-xL during terminal erythroid differentiation. Blood 102:712–717.

Baier A, Meineckel I, Gay S, Pap T. 2003. Apoptosis in rheumatoid arthritis. Curr Opin Rheumatol 15:274–279.

Cain SA, Ratcliffe CF, Williams DM, Harris V, Monk PN. 2000. Analysis of receptor/ligand interactions using whole-molecule randomly-mutated ligand libraries. J Immunol Methods 245:139–145.

Da Costa L, Narla G, Willig TN, Peters LL, Parra M, Fixler J, Tchernia G, Mohandas N. 2003a. Ribosomal protein S19 expression during erythroid differentiation. Blood 101:318–324.

Da Costa L, Tchernia G, Gascard P, Lo A, Meerpohl J, Niemeyer C, Chasis JA, Fixler J, Mohandas N. 2003b. Nucleolar localization of RPS19 protein in normal cells and mislocalization due to mutations in the nucleolar localization signals in 2 Diamond-Blackfan anemia patients: Potential insights into pathophysiology. Blood 101:5039–5045.

Davis LS. 2003. A question of transformation: The synovial fibroblast in rheumatoid arthritis. Am J Pathol 162: 1399–1402.

Draptchinskaia N, Gustavsson P, Andersson B, Pettersson M, Willig TN, Dianzani I, Ball S, Tchernia G, Klar J, Matsson H, Tentler D, Mohandas N, Carlsson B, Dahl N. 1999. The gene encoding ribosomal protein S19 is mutated in Diamond-Blackfan anaemia. Nat Genet 21:169–175.

Farkas I, Baranyi L, Liposits ZS, Yamamoto T, Okada H. 1998. Complement C5a anaphylatoxin fragment causes apoptosis in TGW neuroblastoma cells. Neuroscience 86:903–911.

Farkas I, Takahashi M, Fukuda A, Yamamoto N, Akatsu H, Baranyi L, Tateyama H, Yamamoto T, Okada N, Okada H. 2003. Complement C5a receptor-mediated signaling may be involved in neurodegeneration in Alzheimer's disease. J Immunol 170:5764–5771.

Fukushima Y, Asano T, Saitoh T, Anai M, Funaki M, Ogihara T, Katagiri H, Matsuhashi N, Yazaki Y, Sugano K. 1997. Oligomer formation of histamine H2 receptors expressed in Sf9 and COS7 cells. FEBS Lett 409:283–286.

Hamaguchi I, Flygare J, Nishiura H, Brun A, Dahl N, Richter J, Karlsson S. 2003. Proliferation deficiency of multipotent hematopoietic progenitors in ribosomal protein S19 (RPS19)-deficient diamond-Blackfan anemia improves following RPS19 gene transfer. Mol Ther 7: 613–622.

Horino K, Nishiura H, Ohsako T, Shibuya Y, Hiraoka T, Kitamura N, Yamamoto T. 1998. A monocyte chemotactic factor, S19 ribosomal protein dimer, in phagocytic clearance of apoptotic cells. Lab Invest 78:603–617.

Konteatis ZD, Siciliano SJ, Van Riper G, Molineaux CJ, Pandya S, Fischer P, Rosen H, Mumford RA, Springer MS. 1994. Development of C5a receptor antagonists: Differential loss of functional responses. J Immunol 153: 4200–4205.

Laemmli UK. 1970. Cleavage of structural proteins during the assembly of the head of bacteriophage T4. Nature 227:680–685.

Matsson H, Davey EJ, Draptchinskaia N, Hamaguchi I, Ooka A, Leveen P, Forsberg E, Karlsson S, Dahl N. 2004. Targeted disruption of the ribosomal protein *S19* gene is lethal prior to implantation. Mol Cell Biol 24:4032–4037.

Matsuyoshi H, Senju S, Hirata S, Yoshitake Y, Uemura Y, Nishimura Y. 2004. Enhanced priming of antigen-specific CTLs in vivo by embryonic stem cell-derived dendritic cells expressing chemokine along with antigenic protein: Application to antitumor vaccination. J Immunol 172: 776–786.

Nagata S, Nagase H, Kawane K, Mukae N, Fukuyama H. 2003. Degradation of chromosomal DNA during apoptosis. Cell Death Differ 10:108–116.

Neumann E, Barnum SR, Tarner IH, Echols J, Fleck M, Judex M, Kullmann F, Mountz JD, Scholmerich J, Gay S, Muller-Ladner U. 2002. Local production of complement proteins in rheumatoid arthritis synovium. Arthritis Rheum 46:934–945.

Nishimura T, Horino K, Nishiura H, Shibuya Y, Hiraoka T, Tanase S, Yamamoto T. 2001. Apoptotic cells of an epithelial cell line, AsPC-1, release monocyte chemotactic S19 ribosomal protein dimer. J Biochem 129:445–454.

Nishiura H, Shibuya Y, Matsubara S, Tanase S, Kambara T, Yamamoto T. 1996. Monocyte chemotactic factor in rheumatoid arthritis synovial tissue. Probably a cross-linked derivative of S19 ribosomal protein. J Biol Chem 271:878–882.

Nishiura H, Shibuya Y, Yamamoto T. 1998. S19 ribosomal protein cross-linked dimer causes monocyte-predominant infiltration by means of molecular mimicry to complement C5a. Lab Invest 78:1615–1623.

Nishiura H, Tanase S, Sibuya Y, Nishimura T, Yamamoto T. 1999. Determination of the cross-linked residues in homo-dimerization of S19 ribosomal protein concomitant with exhibition of monocyte chemotactic activity. Lab Invest 79:915–923.

Oubrahim H, Chock PB, Stadtman ER. 2002. Manganese (II) induces apoptotic cell death in NIH3T3 cells via a caspase-12-dependent pathway. J Biol Chem 277:20135–20138.

Ricart KC, Fiszman ML. 2001. Hydrogen peroxide-induced neurotoxicity in cultured cortical cells grown in serum-free and serum-containing media. Neurochem Res 26:801–808.

Shibuya Y, Shiokawa M, Nishiura H, Nishimura T, Nishino N, Okabe H, Takagi K, Yamamoto T. 2001. Identification of receptor-binding sites of monocyte chemotactic S19 ribosomal protein dimer. Am J Pathol 159:2293–2301.

Shrestha A, Horino K, Nishiura H, Yamamoto T. 1999. Acquired immune response as a consequence of the macrophage-dependent apoptotic cell clearance and role of the monocyte chemotactic S19 ribosomal protein dimer in this connection. Lab Invest 79:1629–1642.

Shrestha A, Shiokawa M, Nishimura T, Nishiura H, Tanaka Y, Nishino N, Shibuya Y, Yamamoto T. 2003. Switch moiety in agonist/antagonist dual effect of S19 ribosomal protein dimer on leukocyte chemotactic C5a receptor. Am J Pathol 162:1381–1388.

Soruri A, Kim S, Kiafard Z, Zwirner J. 2003. Characterization of C5aR expression on murine myeloid and lymphoid cells by the use of a novel monoclonal antibody. Immunol Lett 88:47–52.

Umeda Y, Shibuya Y, Semba U, Tokita K, Yamamoto T. 2004. Guinea pig S19 ribosomal protein as precursor of C5a receptor-directed monocyte-selected leukocyte chemotactic factor. Inflamm Res (in press).